

Longitudinal Unevenness and Dynamic Axle Loadings on Concrete Block Pavements

M. Huurman

Delft University of Technology, Faculty of Civil Engineering
Delft, The Netherlands

Summary

At the Delft University of Technology a research program is performed to gain more knowledge about the development of permanent deformation, caused by traffic loadings in concrete block pavements. For this research, amongst others, the longitudinal profiles of a large number of in-service concrete block pavements in three major Dutch cities, with a peat, clay and sand subgrade respectively, were measured.

Calculations on the basis of these longitudinal profiles show that, compared to other pavement types, concrete block pavements only offer a limited comfort. Furthermore it is shown that even new, relatively smooth concrete block pavements are subjected to dynamic axle loadings which show a large standard deviation.

Given the large dynamic axle loadings and the sensitivity for permanent deformation of a concrete block pavement it is concluded that traffic contributes to the development of longitudinal unevenness in a (new) concrete block pavement. The forces of this amplification of longitudinal unevenness are determined using vehicle simulation.

The most simple way to show that traffic indeed introduces longitudinal unevenness, is to calculate the driving comfort (IRI) on concrete block pavements for various travelling speeds. These calculations show that at a speed which is in coherence with other traffic (40 to 60 km/h) the comfort is lower than the comfort at other speeds. At speeds in coherence with other traffic the eigenfrequencies of a vehicle equal the frequencies introduced by longitudinal unevenness reinforced by traffic. The limitation in comfort is thus a result of vehicles reacting to unevenness introduced by themselves.

1 Introduction

At the Delft University of Technology a research program is performed to gain more knowledge about the development of permanent deformation, introduced by traffic loadings, in concrete block pavements. This research is concentrated on the development of the rut depth and of the longitudinal variation of this rut depth. The longitudinal variation of the rut depth of course contributes to the longitudinal unevenness of a concrete block pavement, which implies that the research program concerns both the development of transverse unevenness and longitudinal unevenness of concrete block pavements, caused by traffic loadings.

In this paper some calculations on longitudinal profiles of concrete block pavements will be discussed. Based on simulations of a half vehicle, it will be shown that traffic loadings might very well contribute to the development of ruts which show a varying depth over the length of a road section. Such a varying rut depth contributes to the longitudinal unevenness of a section and thus influences the driving comfort as well as the vehicle response (dynamic axle loads).

By calculating the driving comfort (International Roughness Index, IRI) it is shown that there is a relation between the longitudinal profile of a (older) concrete block pavement and the properties of the traffic using it.

2 Measurements

The transverse and longitudinal profiles of 34 concrete block pavements were measured. These 34 sections are located in the Dutch municipalities of Apeldoorn (sand subgrade), Rotterdam (clay/sand subgrade) and Zaanstad (peat subgrade), and show a large variation in age. Most of these sections have a length of more than 102 m, however six sections are shorter. These shorter sections were used earlier by the former Dutch working group "Design of Small Element Pavements" for the development of the current Dutch Design Method for Concrete Block Road Pavements (1).

The transverse and longitudinal profiles of the sections were measured by the ARAN (Automatic Road Analyzer) of the Road and Hydraulic Engineering Division of the Dutch Ministry of Transport, Public Works and Water Management. The ARAN forms an integrated measuring system which uses ultrasonic transmitters and receivers, gyroscopes and accelerometers to measure the surface of a pavement (2). While measuring, with variable speeds up to 90 km/h, the ARAN uses two video cameras to monitor the pavement surface in the two wheel tracks. A third camera gives the view of the driver. Both the videotapes and the data files contain information about the chainage. The data can thus easily be related to the chainage over a section.

On the basis of the measured transverse and longitudinal profiles a number of calculations was performed to get insight into the way how vehicles load concrete block pavements. The calculations mainly consider the interactions between vehicles and longitudinal profiles. A lot of attention is given to the wavelengths at which certain phenomena occur: wavelengths of longitudinal unevenness combined with wavelengths in vehicle responses. The calculations offer insight into the introduction of longitudinal unevenness caused by vehicles.

In this paper two of these calculations (IRI and vehicle simulation), performed on three sections, are discussed. The three sections were selected from the earlier discussed 34 sections on the basis of the seriousness of their longitudinal unevenness (Power Density at a wavelength of 5 m).

The first section, A01 s, is located in Apeldoorn and showed the smoothest longitudinal profile of the sections measured in this municipality.

The second section is located in Rotterdam. This section, R01 c, shows an average longitudinal unevenness considering the measured concrete block pavements. The third section, Z04, is found in Zaanstad and shows a very serious longitudinal unevenness.

3 The International Roughness Index

3.1 Description of the International Roughness Index

The International Roughness Index, IRI, is an index which in one figure gives an impression of the serviceability, in terms of the driving comfort, of a section. This index is calculated on the basis of a simulation of a quarter car, travelling over a measured longitudinal profile at a speed of 80 km/h. The vertical movements of the masses which form this quarter car hereby determine the IRI. Calculation of the IRI thus requires a computer simulation of a quarter car.

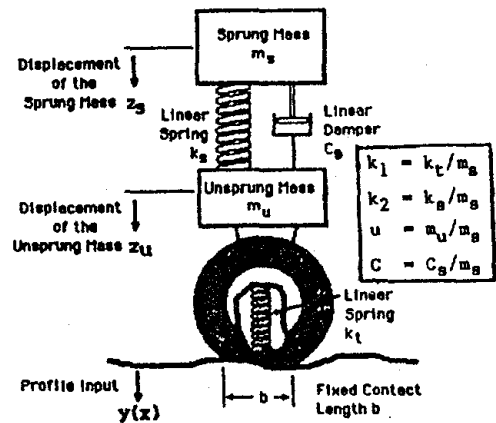


Figure 1 The IRI model of a quarter car (4).

The quarter car to be simulated is formed by a two mass spring system with standardized properties (3, 4). One of the masses represents an axle (or a wheel) and makes contact with the measured longitudinal profile by means of a spring representing the tyre. This mass is called unsprung mass, M_u , see figure 1.

The second mass represents the lorry. This mass is connected to the first one by means of a damper combined with a spring and is called the sprung mass, M_s .

The behaviour of the quarter car is influenced by the weight of these masses, the stiffness of the springs, K_u and K_s , as well as the damper constant, C_s . Since the ratios between these properties determine the vertical movements of the quarter car, these ratios are standardized:

$$\begin{aligned} K_u/M_s &= 653 \quad [N/mkg] & K_s/M_s &= 63.5 \quad [N/mkg] \\ C_s/M_s &= 6 \quad [Ns/mkg] & M_u/M_s &= 0.15 \quad [-] \end{aligned}$$

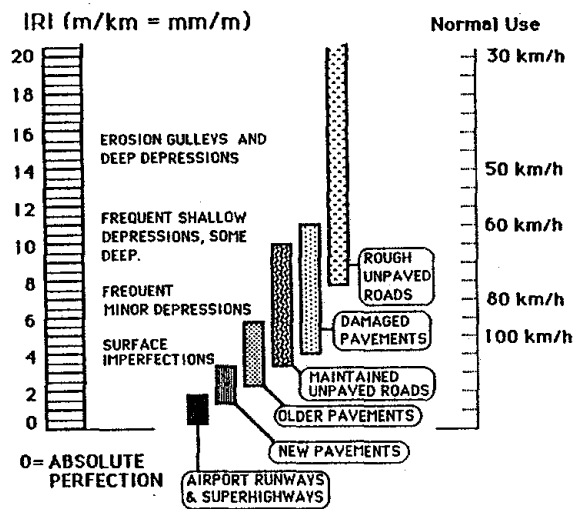


Figure 2 The IRI scale (4).

Calculation of the IRI means that, while simulating the quarter car, the movements in the damper are summed up and divided by the length over which the simulation has been done. The IRI thus is really dimensionless but mostly it is expressed in [mm/m] or [m/km]. The IRI scale of road roughness is given in figure 2.

The IRI does not give a direct measure of the accelerations affecting the riding comfort perceived by users, although it correlates very highly with them (4).

3.2 IRI calculation results

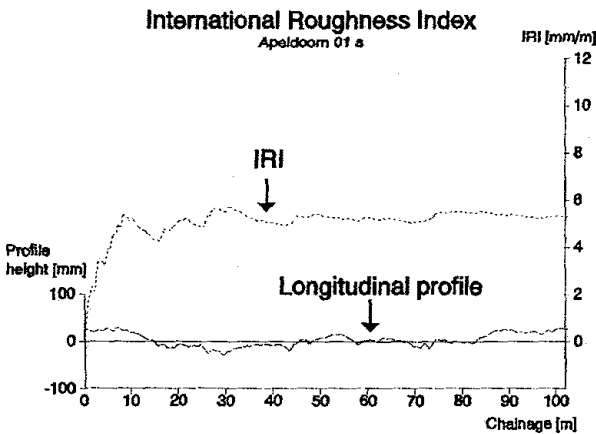


Figure 3 Development of the IRI over the section A01 s. After simulating over 102 m the IRI equals 5.29 mm/m.

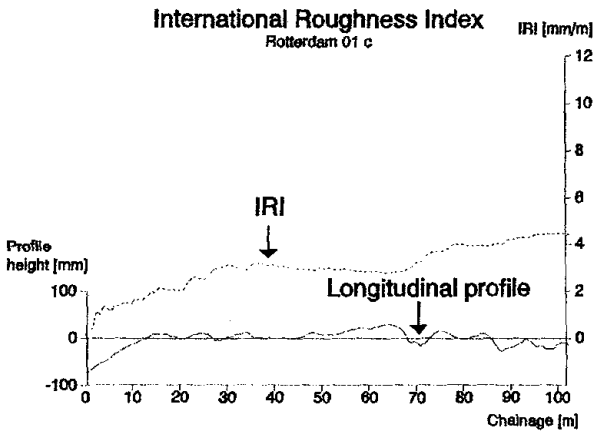


Figure 4 Development of the IRI over the section R01 c. At the end of the section the IRI equals 4.46 mm/m.

The figures 3, 4 and 5 show the development of the IRI, over a length of 102 m for the three sections in the municipalities of Apeldoorn, Rotterdam and Zaanstad respectively.

Comparing the calculated IRI values with the IRI scale (figure 2) one learns that a concrete block pavement with a smooth longitudinal profile (A01 s) results in an IRI which is higher than the IRI of a new (asphalt) pavement. As shown by figure 2 new pavements have IRI values between about 1.25 and 3.25 mm/m.

The smallest IRI determined for all the measured sections equals 3.55 mm/m, while the IRI of a very young, new concrete block pavement in Zaanstad equalled 4.28 mm/m after simulating over a length of about 102 m.

The smoothest measured concrete block pavements thus have an IRI which about equals the IRI of older pavements according to the IRI scale (IRI from about 2.5 to 6.5 mm/m).

The IRI calculated for section Z04 equals 7.02 mm/m, while the largest IRI determined for the measured sections is 7.50 mm/m.

By also relating these values to the IRI scale one learns that old concrete block pavements, showing firm longitudinal unevenness, show a larger IRI than old (asphalt) pavements.

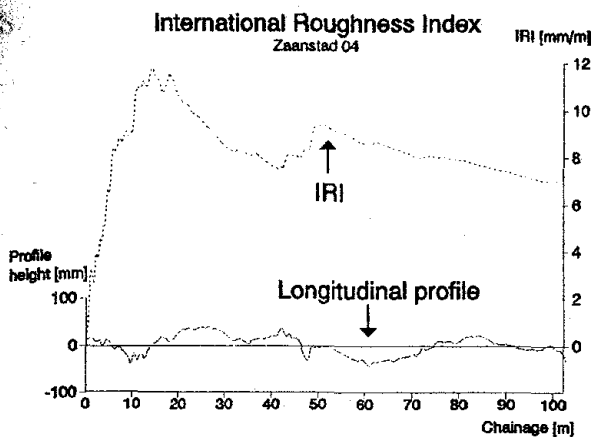


Figure 5 Development of the IRI over the section Z04. At the end of the section the IRI equals 7.02 mm/m.

The highest IRI values determined for the measured concrete block pavements thus are, on the IRI scale, found in the range of damaged pavements or maintained unpaved roads, see figure 2.

IRI calculations thus show that Dutch concrete block pavements are not as smooth as other pavement types (asphalt pavements). Therefore it is expected that the response of vehicles, travelling over these concrete block pavements, will be firm. This will be discussed in the next chapter.

4 Simulation of a half vehicle

4.1 Introduction

In the previous chapter the calculation of the IRI was discussed. It was explained that calculation of the IRI implies the simulation of a quarter car. By expanding the IRI model of a quarter car, a model of a half vehicle (vehicle without width) is obtained. Using this model of a half vehicle, the pitching behaviour (rotation of the lorry around the transverse axis) of a vehicle is accounted for, so that the model becomes more realistic. Using the model of a half vehicle, the longitudinal profile encountered by the front axle influences the dynamic rear axle load.

The model of a half vehicle can be seen as a vehicle without width. This means that the simulation of a half vehicle refers to the responses of a real vehicle travelling over a pavement structure which shows exactly the same longitudinal profiles at both the right and left wheel tracks. The ARAN records a single longitudinal profile based on both the longitudinal profiles at the right and left wheel tracks. This implies that the model of a half vehicle is as realistic as possible when using ARAN data.

4.2 Simulated vehicle

Simulation of a vehicle is only useful when realistic vehicle properties are available. The vehicle properties used in this research program are based on the properties of an existing DAF truck with two axles. The properties of the unladen DAF are retrieved from earlier research performed by Sweere (5, 6).

Based on the properties of this unladen truck the properties of loaded similar trucks can be determined. The vehicle responses which will be discussed in this paper refer to such a loaded DAF truck. This chosen vehicle is loaded by a payload of 6,959 kg which is equally distributed over the load area. At a gravity of 9.8 m/s^2 this vehicle has a static rear axle load of 80 kN.

Properties of the unladen DAF truck:

Ms =	5,500 kg	Ksf =	430,000 N/m
Js =	9,600 kg m ²	Ksr =	700,000 N/m
Muf =	800 kg	Kuf =	1,500,000 N/m
Mur =	1300 kg	Kur =	4,000,000 N/m
Csf =	30,000 Ns/m	Lf =	1.02 m
Csr =	30,000 Ns/m	Lr =	2.18 m

where:

- Ms, Muf, Mur: masses of the sprung mass or lorry, the front unsprung mass or axle and rear unsprung mass or axle respectively
- Ksf, Ksr, Kuf, Kur: stiffness of the springs between the front axle and the lorry, Ksf, between the rear axle and the lorry, Ksr, and the spring stiffness of the front and rear tyres, Kuf and Kur respectively
- Csf, Csr: damper constants of the dampers at the front and rear axle respectively
- Js: moment of inertia of the lorry including payload (if any)
- Lf, Lr: horizontal distance between the centre of gravity of the sprung mass or lorry and the front and rear axle respectively

The payload of the vehicle only influences four of the mentioned vehicle properties: Ms, Js, Lf and Lr. For the chosen loaded vehicle these properties become:

Ms =	12,459 kg
Js =	23,525 kg m ²
Lf =	1.76 m
Lr =	1.44 m

Figure 6 gives an impression of the chosen loaded vehicle. Within this paper the results of vehicle simulation using the properties of this vehicle will be discussed.

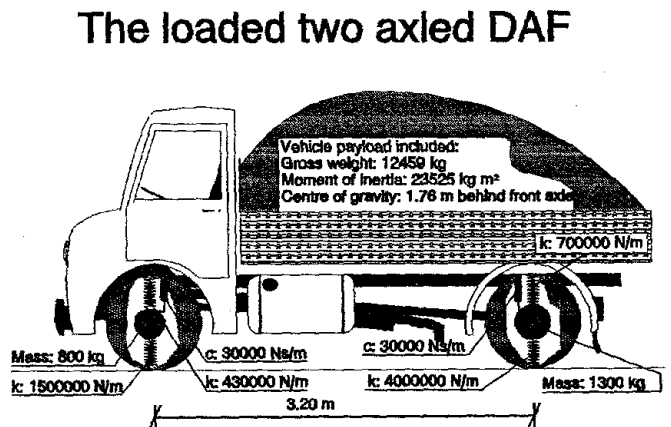


Figure 6 The properties of the loaded two axled DAF truck.

4.3 Dynamic axle loads

The figures 7, 8 and 9 show the results of the simulation of the loaded vehicle travelling over the three sections with a speed of 50 km/h. The figures show that concrete block pavements are subjected to large dynamic axle loads. Some statistics referring to the same dynamic axle loads are given in table 1.

Section	Minimum load [kN]	Maximum load [kN]	Standard deviation [kN]
A01 s	62.09	99.41	6.37
R01 c	51.43	112.13	10.25
Z04	31.41	148.78	13.01

Table 1 Minimum and maximum values and the standard deviation the calculated rear axle load of the chosen vehicle travelling at 50 km/h.

As shown in table 1 the longitudinal unevenness of concrete block pavements causes dynamic axle loads with a large standard deviation. As a result, at some spots on their longitudinal profile, concrete block pavements are subjected to axle loads which are much larger than the static loads of the passing axles.

For instance, the largest dynamic rear axle load on section Z04 is more than 1.85 times the static rear axle load (80 kN).

At other spots on their longitudinal profiles concrete block pavements are subjected to dynamic axle loads which are much smaller than the static axle loads. The smallest dynamic rear axle load of the loaded vehicle travelling over section Z04 at 50 km/h was only 0.39 times the static rear axle load.

Section Z04 resulted in the largest standard deviation of the rear axle load of the loaded vehicle travelling at 50 km/h. The smallest standard deviation found was 5.6 kN which is slightly smaller than the value found for section A01 s. The new concrete block pavement in Zaanstad resulted in a standard deviation of the rear axle load of the loaded vehicle of 6.55 kN.

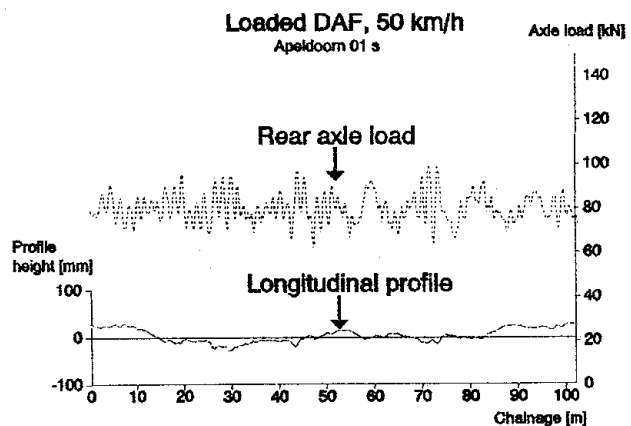


Figure 7 Dynamic rear axle load of the loaded vehicle travelling over section A01 s at 50 km/h.

The smallest dynamic rear axle load of the loaded vehicle travelling over section Z04 at 50 km/h was only 0.39 times the static rear axle load.

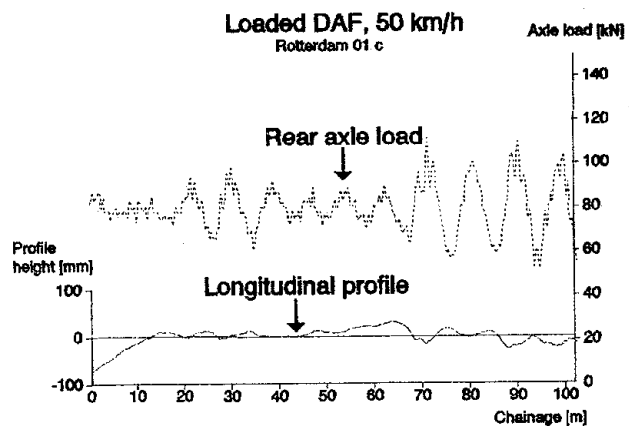


Figure 8 Dynamic rear axle load of the loaded DAF travelling over section R01 c at 50 km/h.

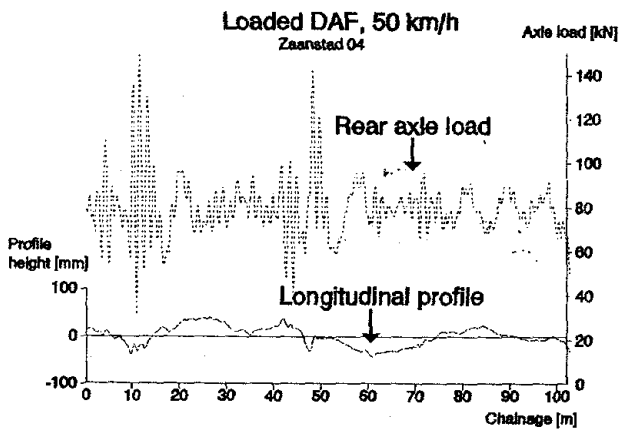


Figure 9 *Dynamic rear axle loaded vehicle travelling over the section Z04 at 50 km/h.*

For section A01 s the smallest dynamic rear axle load of the loaded vehicle equals 0.78 times the static load, the largest dynamic rear axle load equals 1.24 times the static load.

Given these ratios it is concluded that the actual magnitude of the load, which is applied to a concrete block pavement by a single axle, shows a wide range around the static axle load. The width of this range is of course increasing with the amount of longitudinal unevenness of the pavement.

5 Interaction between longitudinal profiles and dynamic axle loads

In chapter 4 it was discussed that concrete block pavements are subjected to dynamic axle loads which show a large standard deviation. Even the longitudinal profiles of new concrete block pavements contain enough longitudinal unevenness to cause a relatively large standard deviation of the dynamic axle loads.

As shown, the dynamic rear axle load of the loaded vehicle is not constant with the chainage. These varying axle loads will introduce a rut depth which will also vary with the chainage, and this varying rut depth will influence the longitudinal profile in the wheel tracks. As a result the longitudinal profile of a section is somewhat altered by a passing vehicle.

If traffic, for instance, introduces high dynamic axle loads at a depression in the initial longitudinal profile of a new concrete block pavement, then the rut depth introduced in this depression will be larger than the mean rut depth of the section. As a result this depression will now deepen with traffic.

The same holds for small dynamic axle loads, if introduced at a hump in an initial longitudinal profile. In this case the rut depth at the hump will be smaller than the mean rut depth, so that the hump is relatively raised by traffic as explained hereafter. If the rut depth varying with the chainage and the initial longitudinal profile are superposed then a new longitudinal profile, slightly formed by traffic, is obtained. The difference between the profile height in the depression and at the hump is now increased as a result of the effects of dynamic axle loads. It might be clear that in this case longitudinal unevenness is reinforced by traffic. Of course dynamic axle loads might also smoothen longitudinal unevenness. This will occur when large dynamic axle loads are introduced at the humps in a longitudinal profile.

In order to get insight into the effects of traffic on the development of longitudinal unevenness in concrete block pavements, the behaviour of vehicles is analyzed using the model of a half vehicle. It was found that the dynamic components of an axle load can be superposed. This implies that the dynamic component of an axle load

caused by a longitudinal profile formed by two perfect sine waves, equals the summed up dynamic components caused by the individual sine waves of unevenness.

Furthermore it was found that the responses of a vehicle to a perfect sine wave form a perfect sine wave too. The wavelengths of both the sine waves are equal and their amplitudes are proportionally related.

A longitudinal profile can be approached by a series of perfect sine waves of unevenness (Fourier series). The vehicle responses to the individual sine waves can be superposed. This implies that the responses of a vehicle to a longitudinal profile are formed by superposing the responses of this vehicle to the individual sine waves within this longitudinal profile.

Based on these findings, the effects of the rear axle of the loaded vehicle on the development of longitudinal unevenness are determined. For this purpose the loaded vehicle is simulated travelling various longitudinal profiles formed by single perfect sine waves of unevenness. The dynamic component of the rear axle load at the deepest spots in such a sine wave of longitudinal unevenness, F_d , is determined. Plotted against the wavelength of the sine waves of unevenness this results in figure 10. As stated, the dynamic component is proportionally related to the amplitude of longitudinal unevenness.

If F_d is positive, then the dynamic rear axle load, at the deepest spots on the sine wave of unevenness, equals the static rear axle load plus F_d times the amplitude of the longitudinal unevenness. The rear axle load at the highest spots on the sine wave of unevenness now is the static rear axle load minus F_d times the amplitude of the unevenness. In this case longitudinal unevenness is amplified by the effects of the rear axle load of the loaded vehicle. The force of this amplification is given in figure 10 and depends on the amplitude of the existing longitudinal unevenness.

If F_d is negative, however, then the situation is opposite, so that existing longitudinal unevenness is smoothed by the effects of the dynamic axle load.

Figure 10 shows two wavelength areas where reinforcement of longitudinal unevenness is expected, that means where F_d is positive. These wavelength areas are related to the eigenfrequencies of the vehicle. The reinforcement of longitudinal unevenness with a wavelength of about 4 to about 10 m is related to the eigenfrequency of the lorry including payload. The positive F_d values at wavelengths of about 0.8 to almost 2 m are related to the eigenfrequency of the rear axle of the loaded vehicle.

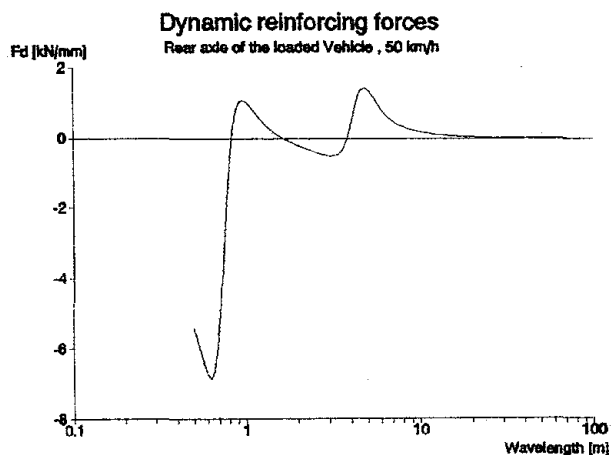


Figure 10 Forces which reinforce existing longitudinal unevenness caused by the dynamic rear axle load of the loaded travelling with a speed of 50 km/h.

Figure 10 shows that longitudinal unevenness with a wavelength shorter than about 0.8 m is smoothed by the effects of the rear axle. A minimum of about minus 7 kN/mm is found at a wavelength of about 0.6 m. Sine waves of longitudinal unevenness with a wavelength of about 0.6 m of course result in an axle load variation. Considering the rear axle of the loaded vehicle, this variation is such that the actual axle loads at the highest spots on these sine waves are increased with 7 kN per mm amplitude (of this unevenness). In the depressions in this unevenness the actual axle loads decreased with 7 kN per mm amplitude. In this case longitudinal unevenness is thus strongly smoothed by the effects of the rear axle of the loaded vehicle.

The responses of a vehicle really depend on the frequencies introduced by the longitudinal profile. This implies that by multiplying the wavelength values on the x-axis by two, one obtains F_d for the rear axle of loaded vehicle travelling with a speed of 100 km/h.

It is clear that the shape of figure 10 depends on the properties of the vehicle as well as its speed. However, similar figures are found for various vehicles. It is therefore expected that real traffic will reinforce and smoothen longitudinal unevenness in a similar manner as discussed here. The absolute values of F_d and the wavelengths at which they are found however depend on the properties and the speeds of the vehicles within real traffic.

6 The effects of traffic on comfort

In the previous chapter it was explained that there are wavelength areas in which traffic is expected to have a smoothing effect on longitudinal unevenness. It was shown that there are also two wavelength areas in which traffic will have a reinforcing effect on existing longitudinal unevenness.

In order to verify the contents of chapter 4 and more particular figure 10, some additional IRI calculations are made. Within these calculations the speed of the IRI quarter car was varied so that the wavelength of longitudinal unevenness for which the IRI vehicle is sensitive varied too, as explained hereafter. It is stated explicitly that calculations of the IRI at other speeds than 80 km/h do not meet the IRI standardization.

Each vehicle has frequencies for which it is very sensitive, eigenfrequencies. These frequencies depend on the various vehicle properties and are determined by the following equation:

$$F_e = \sqrt{K_t/M_t} \text{ [rad/s]} \quad \text{thus} \quad F_e = \frac{\sqrt{K_t/M_t}}{2\pi} \text{ [Hz]}$$

where:

F_e : eigenfrequency of the total mass M_t sprung by springs with a total stiffness K_t

K_t : total stiffness of springs [N/m]

M_t : total sprung mass [kg]

Using this equation the eigenfrequencies of the IRI vehicle become 11 Hz for the unsprung mass or axle and 1.2 Hz for the sprung mass or lorry itself. Similar eigenfrequencies are found for the loaded vehicle, rear axle: 9.6 Hz and loaded lorry: 1.4 Hz.

If the IRI over a section is calculated at various speeds and plotted against the speed at which it was determined it is expected that a plot resembling figure 10 is obtained. At low speeds the eigenfrequencies of the IRI vehicle are triggered by very short waves of longitudinal unevenness. At 1 km/h these wavelengths are 0.025 m and 0.33 m. As shown by figure 10, the effects of the rear axle of the loaded vehicle indicate that traffic will have a smoothing effect on this short waved longitudinal unevenness. Thus at low speeds the IRI vehicle is mainly responding to longitudinal unevenness which is expected to be smoothed by traffic, resulting in minor damper movements. By increasing the speed, the IRI vehicle becomes sensitive to longer waves of unevenness. It will now respond more and more to the reinforced longitudinal unevenness within the wavelength area of about 0.8 m to 2 m, resulting in an increasing IRI.

After the IRI reaches a maximum it is expected to decrease to a minimum at a speed around 17 km/h. At this speed the eigenfrequency of μ is triggered by a wavelength of about 0.4 m. Based on figure 10 it is expected that longitudinal unevenness at this wavelength is smoothed by traffic influences. The eigenfrequency of M_s now correlates with about 3.9 m long waves, which are also expected to be smoothed by the effects of traffic.

A further increase of the speed will increase the IRI too. At a speed of around 35 km/h a second maximum is expected. At this speed the eigenfrequencies of the IRI vehicle correlate with wavelengths of about 0.9 m and about 8 m. As shown by figure 10 longitudinal unevenness with these wavelengths is expected to be reinforced by traffic, resulting in a high IRI.

After reaching its second maximum the IRI is expected to decrease with increasing speed.

Figure 11 gives the movements in the damper of the IRI vehicle determined at various simulated speeds of the IRI quarter car. It is clear that this figure is not in complete coherence with the previous discussion. Maxima and minima are found at larger wavelengths than expected on the basis of figure 10.

This discrepancy might be a result of real traffic travelling over the concrete block pavements with a speed greater than the 50 km/h, on which figure 10 was based. Of course this discrepancy might also be a result of a mismatch between the combined effects of the real vehicles within traffic and the effects of the rear axle of the loaded vehicle.

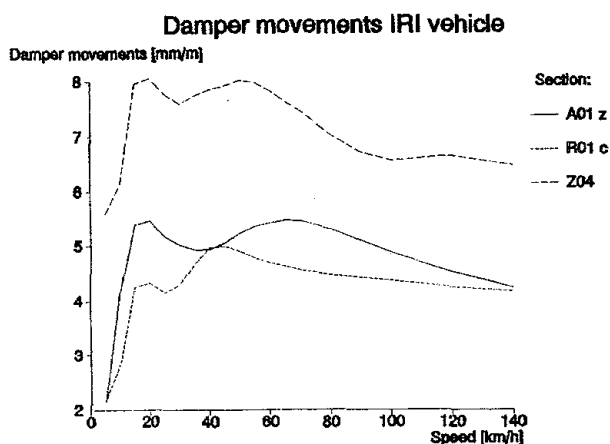


Figure 11 The damper movements of the IRI vehicle per travelled distance, plotted against the simulated speed.

Apart from the differences in the speeds at which the maxima are found, figure 11 clearly shows the form which was expected on the basis of the previous discussion and figure 10. It is therefore concluded that traffic not only introduces transverse but also longitudinal unevenness to a concrete block pavement.

The IRI is expressing the damper movements per travelled distance. The damper movements per second, as a result, show a proportional increase with speed if the IRI remains constant.

7 Conclusions

Concrete block pavements are subjected to dynamic axle loads which show a large standard deviation. The dynamic axle load of a vehicle shows maxima and minima when plotted against the chainage. This will of course result in a rut depth varying with the chainage too, so that the longitudinal profile of a concrete block pavement is somewhat altered by the dynamic axle loads.

By processing the magnitude as well as the phase of the dynamic rear axle load of the chosen loaded vehicle with regard to longitudinal unevenness, the expected effects of this axle on the development of longitudinal unevenness are determined. It is shown that the effects of a dynamic axle load can either reinforce or smoothen existing longitudinal unevenness, depending on the wavelength. The forces of this reinforcing or smoothing of longitudinal unevenness depend on the properties of the vehicles travelling over the pavement and vary with the wavelength of unevenness. These forces can either be positive (reinforcing effect) or negative (smoothing effect) and can be determined on the basis of vehicle simulation.

On the basis of this exercise it was concluded that traffic contributes to the development of longitudinal unevenness in two wavelength areas.

A verification on the basis of numerous simulations of the IRI vehicle travelling at various speeds, showed that traffic is indeed contributing to the development of longitudinal unevenness in concrete block pavements. As a result of the variation of the reinforcing effects of traffic on the development of longitudinal unevenness with the wavelength, the comfort offered by a concrete block pavement depends on the travelling speed. Vehicles travelling at a speed which is in coherence with other traffic vehicles using the concrete block pavement are sensitive to the longitudinal unevenness they introduce themselves. This results in a decrease of comfort as indicated by an increase of the damper movements of the IRI quarter car.

8 Literature

1. Houben, L.J.M. et al.
The Dutch design method for concrete block road pavements
Proceedings Third International Conference on Concrete Block Paving
Rome, 1988, pp. 156 - 169.
2. Swart, J.H., de Wit, L.B.
Travelling computer replaces visual inspection by feet (in Dutch)
Land + Water, april 1990, pp. 40 - 45.

3. Sayers, M.W., Gillespie, T.D., Paterson, W.D.O.
Guidelines for Conducting and Calibrating Road Roughness Measurements
World Bank Technical Paper number 46, The World Bank, Washington, D.C.,
U.S.A., 1986.
4. Paterson, W.D.O.
Road Deterioration and Maintenance Effects - Models for Planning and
Management
The Highway Design and Maintenance standards series
John Hopkins University Press, Baltimore, Maryland, December 1987.
5. Sweere, G.T.H., Elzenaar, J., Harkema, D.A.J.
Vehicle simulation on the hybrid calculation-device AD4 - IBM 1800 (in Dutch)
Report WB-18 (7-80-115-11), Road and Railroad Research Laboratory,
Delft University of Technology, april 1980.
6. Sweere, G.T.H., Molenaar, A.A.A.
Driving comfort and Dynamic axle loads with regard to the longitudinal road
profile (in Dutch).
Report WB-19 (7-80-115-12), Road and Railroad Research Laboratory,
Delft University of Technology, may 1980.
7. Houben, L.J.M.
Small element pavements (in Dutch)
Lecture notes, Delft University of Technology, 1989.

Ir. M. Huurman
Faculty of Civil Engineering
Delft University of Technology
P.O. Box 5048
2600 GA Delft, The Netherlands

Phone +31.15.782763
Telefax +31.15.786993